Thrust Area 4: Solar (Advanced PV Device Program)

Research to Improve Photovoltaic (PV) Cell Efficiency by Hybrid Combination of PV and Thermoelectric Cell Elements

PIs: Nicoleta Sorloaica-Hickman**,** Robert Reedy
Student: Kris Davis

Description: Photovoltaic/thermoelectric (PV/TE) cell integration is a promising technology to improved performance and increase the cell life of PV cells. The TE element can be used to cool and heat the PV element, which increases the PV efficiency for applications in real-world conditions. Conversely, the TE materials can be optimized to convert heat dissipated by the PV element into useful electric energy, particularly in locations where the PV cell experiences large temperature gradients, i.e. use the thermoelectric module for cooling, heating and energy generation depending on the ambient weather conditions. Thus, the goal of this research effort is to research and develop nanoscale design of efficient thermoelectric material through a fundamental understanding of the materials properties and to design and build a photovoltaic thermoelectric (PV/TE) hybrid system.

Budget: $167,820
Universities: UCF/FSEC

Progress Summary

Photovoltaic/Optical/Thermoelectric Device- Unconventional architectures for low cost solar device with high efficiency due to the light capture and conversion

Thus, the goal of this research effort is to research and develop nanoscale design of efficient thermoelectric material through a fundamental understanding of the materials properties and to design and build a photovoltaic thermoelectric (PV/TE) hybrid system.

The realization of a high efficiency/low cost solar hybrid device which is easily manufacturable is one of the defining problems of photovoltaics. Our innovation is to design an integrated optical/PV cell hybrid system allowing efficiency improvements while decreasing the costs, and hence expand the applications for solar energy. It utilizes a design approach which focuses first on performance, enabling the use of old or new photovoltaic materials. The flexibility of these architectures allows a wide portal to accommodate new breakthrough concepts because the device accepts light at wide angles from a large fraction of the sky and it is therefore able to capture most of the diffuse light, which makes up ~10% of the incident power in the solar spectrum.

The PV device consists of many cylindrical cells imbedded into a polymeric matrix with nanoparticles which scatter the light back into the cells. The key optical elements which enhance the light capture are: light trapped by the glass/polymer fiber, light transmitted through the transparent electrodes (ITO and graphene), light absorbed and scattered by the nanoparticles imbedded into the polymeric matrix and, light reflected back into the device by the metallic substrate.

The key electrical elements which enhance the light conversion are photo-excited electrons and holes traveling very short distances before being collected by the electrodes. This concept could decrease the electronic recombination caused by impurities, high anti-reflection and high surface energy which could increase EQE.

FSEC researchers have fabricated high efficiency and low cost unconventional cylindrical architecture solar devices for terrestrial applications by combining the solar cell design with a novel optical design. This approach allows multiple benefits including: decreasing the amount of active semiconducting materials to less than 5%, increasing the light absorption and conversion, improved performance with non-ideal (lower cost) materials, increased flexibility of the material choices and increase the overall efficiency. The concept is being demonstrated using organic materials (P3HT/PCBM) and a similar platform as used for high performance inorganic solar cells. The process uses inexpensive fabrication technologies which could define a new direction in the PV large-scale fabrication of this PV/optical device.

2011 Annual Report

FSEC researchers have fabricated high efficiency and low cost unconventional cylindrical architecture solar devices for terrestrial applications by combining the solar cell design with a novel optical design. This approach allows multiple benefits including: decreasing the amount of active semiconducting materials to less than 5%, increasing the light absorption and conversion, improved performance with non-ideal (lower cost) materials, increased flexibility of the material choices and increase the overall efficiency. The concept is being demonstrated using organic materials (P3HT/PCBM) and a similar platform as used for high performance inorganic solar cells. The process uses inexpensive fabrication technologies which could define a new direction in the PV large-scale fabrication of this PV/optical device.

The realization of a high efficiency/low cost solar hybrid device which is easily manufacturable is one of the defining problems of photovoltaics. Our innovation is to design an integrated optical/PV cell hybrid system allowing efficiency improvements while decreasing the costs, and hence expand the applications for solar energy. It utilizes a design approach which focuses first on performance, enabling the use of old or new photovoltaic materials. The flexibility of these architectures allows a wide portal to accommodate new breakthrough concepts because the device accepts light at wide angles from a large fraction of the sky and it is therefore able to capture most of the diffuse light, which makes up ~10% of the incident power in the solar spectrum.

Unconventional architectures: Photovoltaic/Optical Device

The PV/Optical glass rod cell consists of four layers deposited on a very thin glass or polymer fiber: a transparent anode shell, a positively charged/doped shell; a negatively charged/doped shell and a transparent cathode shell. [1] (fig.1) The light is incident on the fiber and cell and it is transmitted down the fiber and reflected multiple times from its interior surface, until passing through the active layers and absorbed or passed through the transparent electrodes, thus allowing for multiple passes through active layers of the incident or adjacent cells. Two metal layers separated by a dielectric material are used to collect the photo-generated charges. They constitute the device back side of the PV/optical hybrid device. The electrode shells of each cell are of different length, with the outer and shorter electrode shell connected to the upper metal layer, and the longer inner electrode shell passing through the dielectric layer and connecting to the lower metal layer. One of the metal layers is connected to the positively charged transport electrode and the second metal is connected to the negatively charged transport electron.

The PV device consists of many cylindrical cells imbedded into a polymeric matrix with nanoparticles which scatter the light back into the cells.[2] (fig.2)The key optical elements which

enhance the light capture are: light trapped by the glass/polymer fiber, light transmitted through the transparent electrodes (ITO and graphene), light absorbed and scattered by the nanoparticles imbedded into the polymeric matrix and, light reflected back into the device by the metallic substrate.

The key electrical elements which enhance the light conversion are: photo-excited electrons and holes traveling very short distances before being collected by the electrodes, which could decrease the electronic recombination caused by impurities, high anti-reflection, high surface energy which could increase EQE. [3]

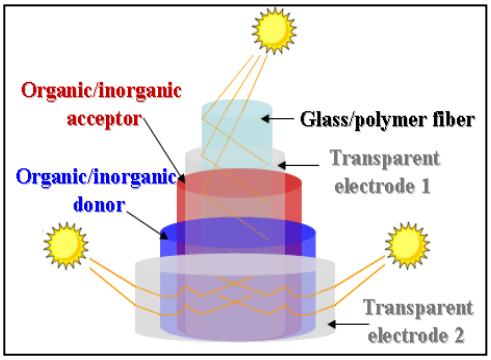

Figure 1: Rod and multifunction tube PV cells

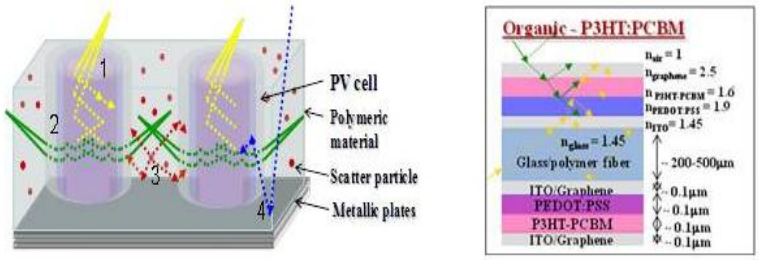

Figure 2. Schematic of the PV/optical device

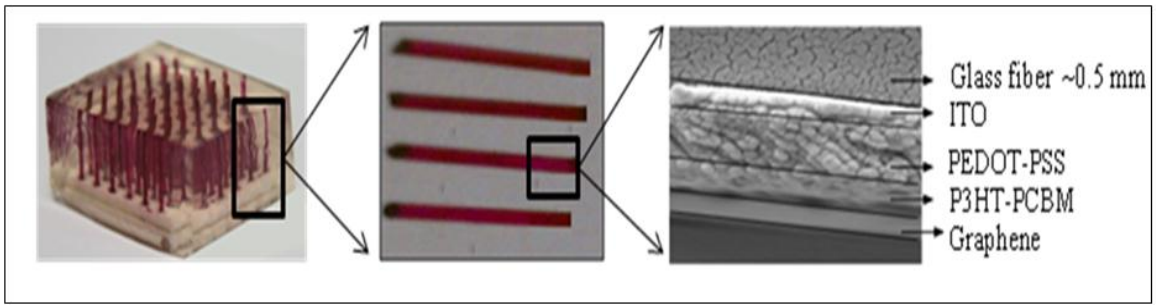

Figure 3: PV device

The first step in building the PV/Optical device was to fabricate and optimize the optical and electrical properties of the transparent graphene electrodes. They are the key elements in achieving high efficiency PV/Optical device.

Transparent electrodes fabrication and results:

GO can be readily obtained from exfoliation of graphite through oxidation. A stable 0.5 mg/mL GO aqueous dispersion (GO ethanol dispersion) was obtained by adding GO into DI water (ethanol) followed by 1 h (3 h) sonication. In order to achieve a highly uniform deposition, we employed a motor controlled two dimension airbrush spray coating system to deposit the GO dispersion onto a preheated glass substrate at about 70 ^{o}C. The moving speed of air brush is set as 19 mm/s. Spray rate is about 3-10 μL/s, controlled by the pressure of N_2. The GO coatings in different thickness were achieved by controlling the runs of spray. The as prepared GO coatings were covered by quartz glass, then, reduced by 6 h UV radiation under a 40 W UV light and followed by annealing under Ar atmosphere at 400 ^{o}C for 30 min.

Optical properties of sprayed GO coatings and RGO coatings were studied. The GO coatings showed very high light transmittance. Even GO coating sample with 8 runs spray still gave a transmittance around 80% (Fig.5) at 550 nm. After reduction, the transmittance of graphene could show a decrease. For example, a 92% transmittance was observed on the 4 runs spray coating GO sample. After UV reduction, the transmittance dropped to 65%. Then, a slight decrease was also observed after the thermal reduction, resulting into a 63% transmittance. We also noticed there is a slight increase of the transmittance at UV band (below 360 nm), which is very interesting. It might be explained that the electronic conjugation within graphene sheets was further restored by the thermal reduction, which caused a redshift of the absorption peak and a change of the intensity at UV band [5]. Drop coating and spin coating methods were attempted in the deposition of GO coatings. However, these experiments all resulted in uneven GO platelets as water (H2O) or ethanol (EtOH) evaporated and GO concentrated. Only spray coating on hot substrate generate a uniform coating that show almost the same transmittance spectra at different position of one GO Coating. It might be explained that the small droplets and immediate evaporation prevented the GO platelets from aggregating.

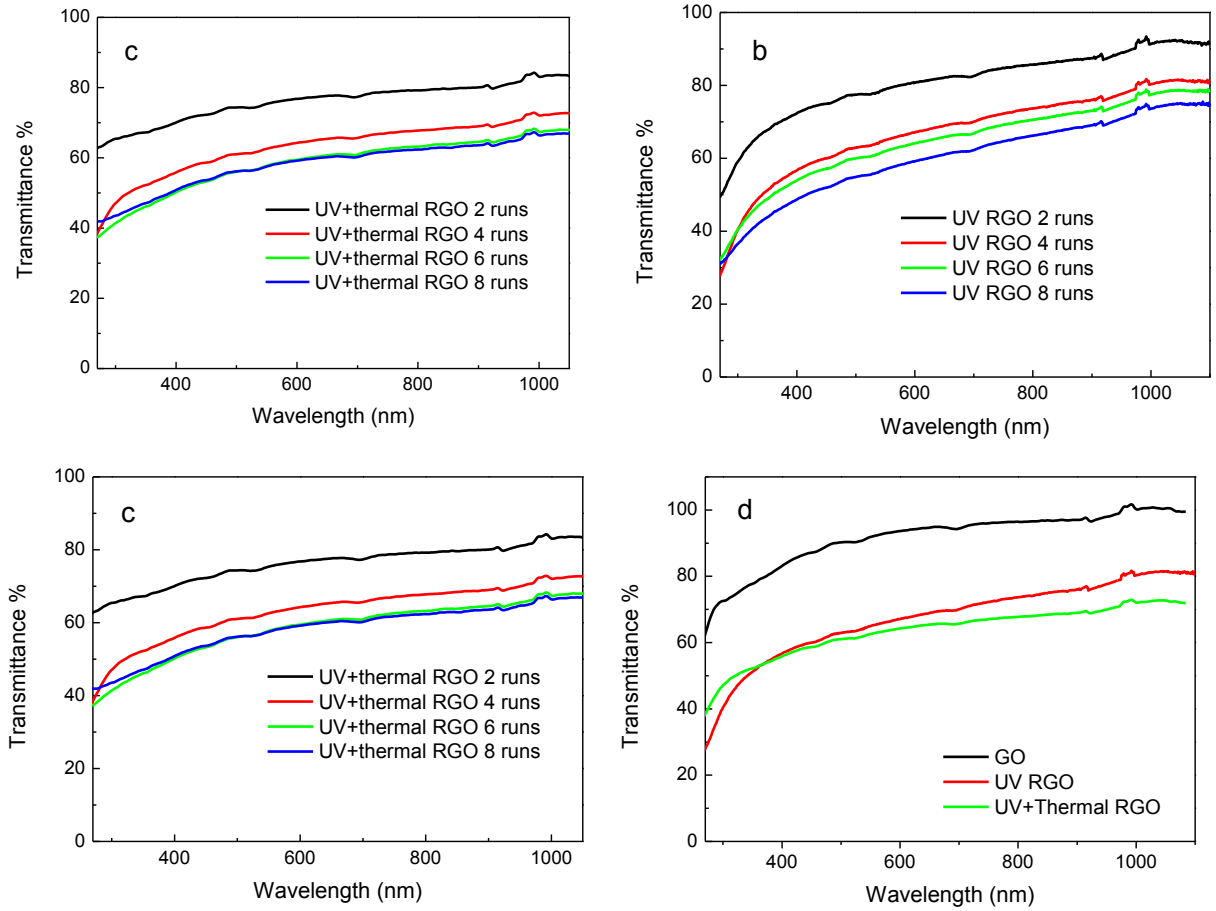

Fig. 5: Transmission spectra of GO coatings with 2, 4, 6 and 8 run sprayed with GO/H_2O. (a, GO coatings. b, UV treated RGO coatings. c, UV+thermal treated RGO coatings). d, Transmission of 6 runs GO coating before and after treated.

Raman spectra of the GO film before and after the reduction process are shown in Fig. 6. Of particular interest is the disorder-induced characteristic Raman 'D' peak at around 1340 cm−1 [6] and a broad G-band at 1580 cm-1, the latter corresponding to the first-order scattering of the E2g mode [7,8]. Another peak at 2940 cm−1, close to the second-order features such as 'D + D' [9] or 'D + G' [10], is also observed. The 2D peak is too weak in intensity to be observed. The prominent D peak is from the structural imperfections created by the attachment of hydroxyl and epoxide groups on the carbon basal plane. After UV and heat treatment, the magnitude of D band peak dropped, and the ID/IG ratio decreased from 0.755 to 0.708, which indicates a reduction of the GO film[11]. The behavior of ID+D'/IG (dropping from 0.237 to 0.192) also shows a matching result.

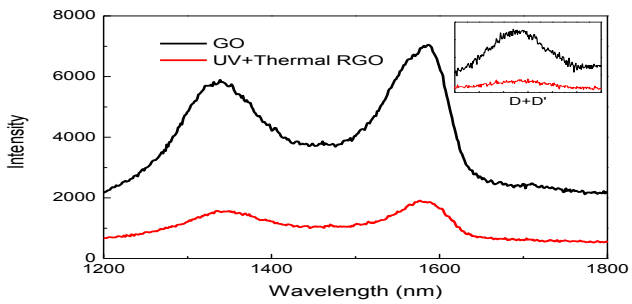

Fig. 6. Raman spectra of D and G band, with inset showing the D+D' band for 6 run spray coating GO and RGO films.

Fig. 7 shows the SEM images of RGO films sprayed with GO/H2O (Fig 7a-d) and GO/EtOH dispersions (Fig 7e-h). The SEM image of hydrazine vapor treated RGO film (Fig.7a) indicates a homogeneous morphology of graphene coatings. Graphene exhibits typical wrinkled structure with corrugation and scrolling which is intrinsic to graphene, whick may be important for preventing aggregation of graphene due to van der Waals forces during drying and maintaining high surface area[12,13]. On the image of 200 oC thermal treated RGO in standard N2 atmosphere (Fig.7b), micro aggregations were observed forming the shape of small water droplets. It suggests the GO might aggregate slightly when the small water droplet dries. Some graphene pieces were also found on the RGO film. When heating to 400 oC under standard N2, the RGO film was burned by the small amount of oxygen in the standard N2 (Fig.7c). Fig.3d shows the RGO film treated by UV and 400 oC heating under pure Ar (99.999%). Structures like water droplets were still observed, and small pieces of graphene were also found on the RGO film.

Structures of droplets were not found in fig 7e. The RGO film looks very smooth and clean with only a small amount of isolated graphene pieces on it. Since ethanol evaporates faster than water, we employed bigger ethanol droplets to form a very thin ethanol film during the spray process. At about 70 oC, the ethanol film dried very fast on the glass substrate and the GO did not concentrate, generating a very homogenous GO film. However, it is difficult to dry a thin water film immediately, even at a higher temperature. A few droplet structures were found on the film sprayed with smaller droplets (fig 7f). Also, more isolated graphene pieces were observed. The RGO samples with thinner films (fig 7g, h) showed uneven and discontinuous RGO film. Single layer graphene films were observed here.

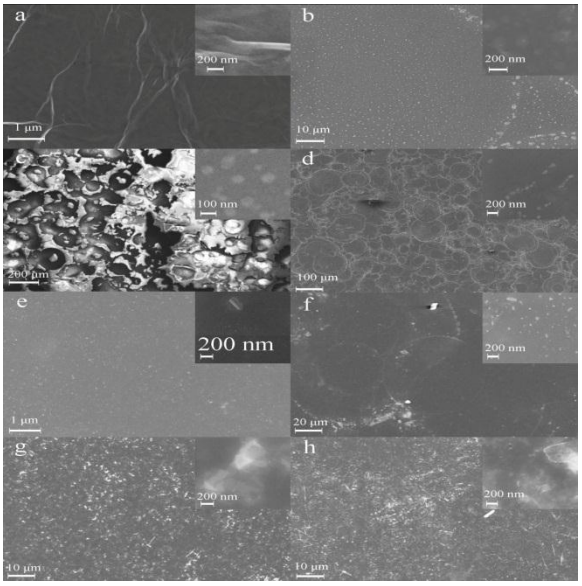

Fig. 7: TEM images of RGO coatings treated by a, Hydrazin. b, 200 ^{o}C, N_2. c, 400 ^{o}C, N_2. d-h, 400 ^{o}C, Ar. (Spray setting: a-d, sprayed in 5 μL/s for 8 runs with GO/H_2O dispersion. e, sprayed in 10 μL/s for 5 runs with GO/EtOH dispersion. f, sprayed in 7 μL/s for 7 runs with GO/EtOH dispersion. g, sprayed in 5 μL/s for 5 runs with GO/EtOH dispersion. f, sprayed in 3.5 μL/s for 7 runs with GO/EtOH dispersion.)

AFM images were studied to further discover the morphology and measure the thickness of the RGO films (Fig. 8). The image shows RGO film is formed by several layers of graphene and the film is

very smooth even in a large scale (5 μm). By scratching the RGO film, we also measured the thickness as 6 nm.

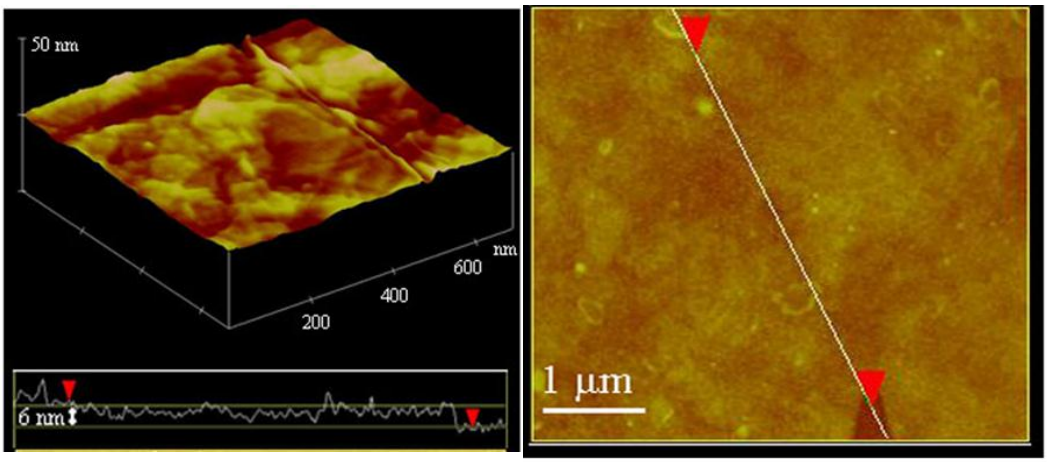

Fig 8: AFM images of RGO films sprayed in 10 μL/s for 5 runs with GO/EtOH dispersion and treated by UV and thermal annealing at 400 ^{o}C Ar.

In summary, we report a method to deposit uniform and controllable GO coatings by spray coating. Homogeneous RGO coatings were achieved by combined reduction with UV and annealing under Ar atmosphere. The graphene coatings show promising applications on transparent and conductive electrodes. We will employ graphene coatings to fabricate the enhanced light harvesting solar cells in further work.

Donor-acceptor fabrication (PEDOT-PSS, P3HT/PCBM):

For standard devices a layer of 0.45 μm filtered PEDOT: PSS was sprayed in a temperature controlled environment onto ITO coated glass fibers which were then annealed at a temperature of 125 °C for 1 minute. A layer of 0.45 μm filtered 1:0.8 P3HT: PCBM was then sprayed forming the active layer of the devices and following that the devices were solvent annealed for 5 minutes. Studies of the thickness and thermal annealing were performed in order to optimize the power conversion efficiency.[4]

References:

[1]. Yuan Li, Eric D. Peterson, Huihui Huang, Mingjun Wang, Dan Xue, Wanyi Nie, Wei Zhou, and David L. Carroll, *Tube-based geometries for organic photovoltaics*, Appl. Phys. Lett. 96, 243505 (2010);

[2]. Joseph Lik Hang Chau, Ruei-Tang Chen, Gan-Lin Hwang, Ping-Yuan Tsai, and Chien-Chu Lin, *Transparent solar cell window module*, Solar Energy Materials and Solar Cells, Volume 94, Issue 3, March 2010, Pages 588-591

[3]. Hsin-Cheng Lee, Shich-Chuan Wu, Tien-Chung Yang and Ta-Jen Yen, *Efficiently Harvesting Sun Light for Silicon Solar Cells through Advanced Optical Couplers and A Radial p-n Junction Structure*, Energies 2010, *3*, 784-802;

[4]. Youngkyoo Kim, Amy M. Ballantyneb, Jenny Nelsonb and Donal D.C. Bradleyb, *Effects of thickness and thermal annealing of the PEDOT:PSS layer on the performance of polymer solar cells*, Organic Electronics, Volume 10, Issue 1, February 2009, Pages 205-209

[5] D. Li, M. B. Müller, S. Gilje, R. B. Kaner, G. G. Wallace. Nature Nanotechnology 3, 101-105 (2008)
[6] A. C. Ferrari. Solid State Commun. 143, 47-57 (2007)
[7] M. Ramm, M. Ata, T. Gross, W. Unger. Appl Phys A: Mater 70, 387–90 (2000)
[8] D. Yang, A. Velamakanni, G. Bozoklu, S. Park, M. Stoller, R. D. Piner, S.Stankovich, I. Jung, D. A. Field, C.A. Ventrice Jr., R. S. Ruoff, Carbon. 47, 145-152 (2009)
[9] T. Gokus, R. R. Nair, A. Bonetti, M. Boehmler, A. Lombardo, K. S. Novoselov, A. K. Geim, A. C. Ferrari, A. Hartschuh, ACS NANO 3, 3963-3968 (2009).
[10] J.Campos-Delgado, J. M. Romo-Herrera, X. Jia, D. A. Cullen, H. Muramatsu, Y. A. Kim, et al Nano Lett. 8, 2773-2778 (2008)
[11] I. Childres, L. A Jauregui, J. Tian, Y. P Chen. New J. Phys. 13, 025008-025020 (2011)
[12] M.J. McAllister, J.L. LiO, D.H. Adamson, H.C. Schniepp, A.A. Abdala, J. Liu, M. Herrera-Alonso, D.L. Milius, R. CarO, R.K. Prud'homme, I.A. Aksay, Chem of Mater. 19, 4396-4944 (2007)
[13] R. Kou, Y.Y. Shao, D.H. Wang, M.H. Engelhard, J.H. Kwak, J. Wang, V.V. Viswanathan, C.M. Wang, Y.H. Lin, Y. Wang, I.A. Aksay, J. Liu, Electrochemistry Communications 11, 954-957 (2009)